BIOCHEMISTRY
including biophysical chemistry & molecular biology

Article

pubs.acs.org/biochemistry

Tandem GA Residues on Opposite Sides of the Loop in Molecular Beacon-like DNA Hairpins Compact the Loop and Increase Hairpin Stability

Chun Yaw (Joel) Chang† and Nancy C. Stellwagen*

Department of Biochemistry, University of Iowa, Iowa City, Iowa 52242, United States

Supporting Information

ABSTRACT: The free solution electrophoretic mobilities and thermal stabilities of hairpins formed by two complementary 26-nucleotide oligomers have been measured by capillary electrophoresis. The oligomers are predicted to form molecular beacon-like hairpins with 5 bp stems and 16 nucleotides in the loop. One hairpin, called hairpin2 (hp2), migrates with a relatively fast free solution mobility and exhibits melting temperatures that are reasonably well predicted by the popular structure-prediction program Mfold. Its complement, called hairpin1 (hp1), migrates with a slower free solution mobility and forms a stable hairpin only in solutions containing ≥200 mM Na^+. The melting temperatures observed for hp1 are ∼18 °C lower than those observed for hp2 and ∼20 °C lower than those predicted by Mfold. The greater thermal stability of hp2 is due to the presence of tandem GA residues on opposite sides of the loop. If the corresponding TC residues in the hp1 loop are replaced by tandem GA residues, the melting temperatures of the modified hairpin are close to those observed for hp2. Eliminating the tandem GA residues in the hp2 loop significantly decreases the thermal stability of hp2. If the loops are replaced by a loop of 16 thymine residues, the free solution mobilities and thermal stabilities of the T-loop hairpin are equal to those observed for hp1. Hence, the loop of hp1 appears to be relatively unstructured, with few base−base stacking interactions. Interactions between tandem GA residues on opposite sides of the hp2 loop appear to compact the loop and increase hairpin stability.

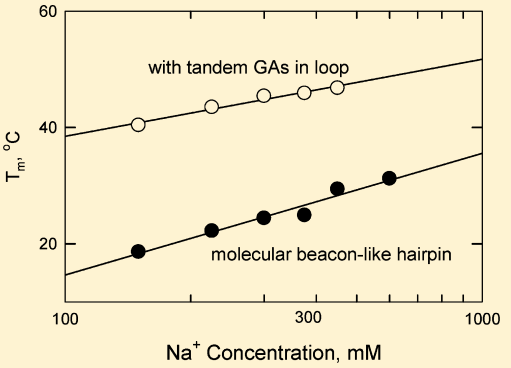

DNA hairpins have become indispensible tools in modern molecular biology and biotechnology. Hairpins with dangling ends are used as capture probes for microarray hybridization[1] and templates for DNA nanodevices (e.g., refs 2−4). DNA hairpins are also used as biosensors, often called "molecular beacons" because they exploit changes in fluorescence to monitor substrate−target interactions.[5−8] Molecular beacons usually have relatively short, marginally stable stems and relatively long loops containing a sequence complementary to that of a target of interest. Hybridization of the loop to the target opens the hairpin and leads to a change in fluorescence, which can be measured. For these and other applications, it is important to be able to predict the stabilities of DNA hairpins and duplexes with different sequences under a variety of experimental conditions.

Current structure-prediction algorithms use the nearest neighbor model to estimate the melting temperatures of DNA (and RNA) hairpins and duplexes.[9−11] The thermal stabilities of model duplexes have usually been measured in solutions containing 1 M NaCl and are scaled to other ionic strengths by using various predictive equations.[12−14] The algorithms work reasonably well to predict the melting temperatures of DNA duplexes and duplexes with single mismatches, because the observed melting temperatures usually agree with the melting temperatures predicted by Mfold within ∼2 °C.[12,15−18] However, the database of nearest neighbor energy parameters contains relatively few examples of the sequence-dependent stabilities of DNA oligomers containing hairpins, bulges, and large internal loops, making the thermodynamic rules predicting the stabilities of such oligomers less certain.[12]

DNA thermal stabilities have been measured by a variety of methods, including UV absorption, fluorescence, and calorimetry (e.g., refs 9−21). Another technique that has been used to monitor DNA conformation is capillary electrophoresis (CE).[22−24] The free solution mobility of a small DNA oligomer is determined by the ratio between its effective charge and its frictional coefficient.[25] When a small DNA hairpin or duplex is denatured by temperature or chemical reagents, the conformation becomes less compact, increasing the frictional coefficient while the effective charge remains approximately constant. Hence, the mobility of a hairpin (or duplex) will decrease with increasing temperature or denaturant concentration until it becomes approximately equal to that of a random coil containing the same number of nucleotides.[22−24] The decrease in the free solution mobility with increasing

Received: August 10, 2011
Revised: September 22, 2011
Published: September 23, 2011

Table 1. Names and Sequences of Molecular Beacon-like Hairpins Used in This Study, Their Melting Temperatures Observed in Solutions Containing 225 mM Na^+, Their Melting Temperatures Predicted by Mfold[a] under the Same Conditions, and Their Mobilities Observed at 20 °C in BGEs Containing 225 mM Na^+

Acronym	Sequence [b,c]	$T_{m,obs}$ [d]	$T_{m,pred}$ [a]	Mobility, m.u. [e]
hairpin1 (hp1)	CGTAA-AATCTATCAAAATCTA-TTACG	22	40	1.986
hp1-stable-stem	**GCGAG**-AATCTATCAAAATCTA-**CTCGC**	45	56	2.097
hp1-TT-loop-close	CGTAA-**T**ATCTATCAAAATCT**T**-TTACG	30	38	2.098
hp1-GC-stem-close	C**A**TA**G**-AATCTATCAAAATCTA-**CTA**TG	32	32	2.024
hp1-2GA	CGTAA-AA**GA**TATCAAAA**GA**TA-TTACG	44	40	2.149
hp1-1GA	CGTAAAA**GA**T-ATCAAA-ATCTATTACG	51	52	2.206
hp1-no-beacon	**GC**TAAAATCTATCAAA-ATCTA-TTACG	--	9	1.88 [f]
hairpin2 (hp2)	CGTAA-TAGATTTTGATAGATT-TTACG	40	38	2.142
hp2-AA-loop-close	CGTAA-**A**AGATTTTGATAGAT**A**-TTACG	39	39	2.120
hp2-2TC	CGTAATA**TC**-TTTT-GATA**TC**TTTTACG	43	42	2.095
hp2-3G	CGTAA-T**GGG**TTTTGAT**GGG**TT-TTACG	31	38	2.046
T-loop	CGTAA-**TTTTTTTTTTTTTTTT**-TTACG	25	38	1.971
T26	TTTTTTTTTTTTTTTTTTTTTTTTTT	--	--	1.754

[a]Melting temperature predicted by Mfold.[30,31] The estimated accuracy is ±2 °C.[12] [b]Changes from the sequences of the parent hp1 and hp2 hairpins are indicated in bold. [c]The hairpin loops in the most stable structure predicted by Mfold for each hairpin are enclosed between hyphens. The Mfold-predicted structures of all hairpins are illustrated in Figure S1 of the Supporting Information. [d]The estimated uncertainty in the observed melting temperatures is ≤1 °C. [e]The estimated uncertainty of the mobilities is ±0.003 mobility unit. [f]Estimated from mobilities measured in BGEs containing 150 and 300 mM Na^+ ions.

temperature or denaturant concentration is therefore a direct measure of the helix−coil transition. Gel electrophoresis can be used to monitor DNA denaturation in a similar manner.[26,27] However, CE measurements are not complicated by possible DNA−matrix interactions[28,29] that might perturb the conformational equilibrium. In addition, the CE measurements are relatively fast, and each experiment requires very little sample.

We have previously measured the free solution mobilities and melting temperatures of single-stranded DNA oligomers containing 26-nucleotides and found that the free solution mobilities observed at 20 °C were correlated with hairpin formation.[23] Oligomers that exhibited relatively slow mobilities at 20 °C were random coils that did not undergo a conformational transition with increasing temperature. By contrast, oligomers that exhibited intermediate or fast mobilities at 20 °C exhibited mobilities that decreased sigmoidally with increasing temperature, indicating that they were hairpins that became denatured at high temperatures. In many cases, oligomers with complementary sequences exhibited similar mobilities at 20 °C and similar melting temperatures, especially if the oligomers were GC-rich. However, if two complementary oligomers were AT-rich, they often exhibited very different free solution mobilities and thermal stabilities, suggesting that one complement formed a stable hairpin while the other strand was a random coil under the same conditions.[23]

In this report, we describe a detailed study of two complementary oligomers containing 73% A+T, called hairpin1 (hp1) and hairpin2 (hp2) for the sake of brevity. The two oligomers have palindromic ends and exhibit significantly different mobilities in 40 mM Tris buffers at 20 °C, suggesting that one forms a hairpin under these conditions while the other does not. The popular structure-prediction program Mfold[30,31] predicts that hp1 and hp2 form similar molecular beacon-like hairpins with 5 bp in the stem and 16 nucleotides (nt) in the loop. Mfold also predicts that hp1 should be slightly more stable than hp2. However, the results indicate that the melting temperature of hp1 is ∼18 °C lower than that observed for hp2 and ∼20 °C lower than that predicted by Mfold. The melting transitions observed for sequence variants of the two hairpins suggest that the difference in stability is due primarily to the fact that the hp1 loop is relatively unstructured while the hp2 loop is compacted by interactions between tandem GA residues located on opposite sides of the loop. Loop compaction therefore appears to be an implicit assumption in the Mfold algorithm.

MATERIALS AND METHODS

DNA Samples. All DNA oligomers were synthesized by Integrated DNA Technologies (Coralville, IA), purified by denaturing polyacrylamide gel electrophoresis, and characterized by mass spectrometry. The acronyms and sequences used for hp1, hp2, and their sequence variants are given in the first two columns of Table 1. Modified nucleotides in the hp1 and hp2 sequence variants are indicated in bold. The most stable hairpin structure predicted for each oligomer by Mfold[30,31] is indicated by hyphens separating the stem and loop residues. The most stable structures predicted by Mfold for the various hairpins are also illustrated in Figure S1 of the Supporting Information. An oligomer containing 26 thymine residues, called T26, was used as an unstructured random coil control. Stock solutions containing each DNA at 1 μg/μL were prepared in 10 mM Tris-acetate buffer (pH 8.0) and stored at −20 °C until they were needed. Aliquots of the stock solutions were mixed as desired and diluted 10-fold with deionized water for the CE measurements. Unless otherwise indicated, the hairpin concentration used in the melting experiments was 1.2×10^{-5} M. The concentration of $Tris^+$ ions in the injected solutions was 0.5 mM, negligible in comparison to the concentration of Na^+ in the background electrolytes (BGEs) used for electrophoresis.

Buffers. Melting experiments were conducted in BGEs containing diethylmalonate (DM) as the buffering anion and Na^+ as the cation. Stock solutions containing 0.5 M diethylmalonic acid [$(CH_3CH_2)_2C(COOH)_2$ (Sigma-Aldrich, St. Louis, MO)] were titrated to pH 7.3, the pK_a of the second

dx.doi.org/10.1021/bi201263n|Biochemistry 2011, 50, 9148−9157

carboxyl group, with a concentrated solution of NaOH. The ionic strength of the buffer stock solution was 1.0 M; the Na^+ concentration was 0.75 M, because the second carboxyl group of diethylmalonic acid is half-ionized at pH 7.3. Aliquots of the buffer stock solution were diluted to the desired concentration before each CE measurement. To avoid confusion in the following text, the cation concentration in each BGE refers to the concentration of Na^+ ions, not the concentration of the buffering anion.

Capillary Electrophoresis. Capillary zone electrophoresis measurements were taken with a Beckman Coulter (Fullerton, CA) P/ACE System MDQ capillary electrophoresis system run in reverse polarity mode (anode on the detector side) with UV detection at 254 nm, using procedures described previously.[24,32,33] The capillaries (Polymicro Technologies, Phoenix, AZ) were 30.9 ± 0.2 cm in length (20.6 ± 0.2 cm to the detector) and 75 μm in internal diameter, coated internally with linear polyacrylamide to minimize the electroosmotic flow (EOF) of the solvent. Previous studies have shown that internal polyacrylamide coatings do not affect the observed mobilities.[34] The capillaries were mounted in a liquid-cooled cassette for good thermal control.

The electric fields used for the experiments ranged from 25 to 175 V/cm, depending on the temperature and conductivity of the BGE; the current in the capillary was generally less than 60 μA. The DNA samples were injected hydrodynamically at a low pressure (0.5 psi, 0.0035 MPa) for 3 s. The injection volume was ~22 nL, giving a sample plug that occupied ~2.6% of the capillary length. Control experiments have shown that the mobilities measured under these conditions are independent of DNA concentration, the length of the sample plug, and the electric field strength.[34]

The free solution mobility of an analyte, μ, is determined by the ratio between its effective charge, Q, and its frictional coefficient, f, as shown in eq 1:[25]

$$\mu = Q/f \tag{1}$$

The mobilities are calculated from the migration times and the applied electric field strength, according to eq 2:

$$\mu_{obs} = L_d/Et \tag{2}$$

where μ_{obs} is the observed mobility, L_d is the distance from the inlet to the detector (in centimeters), E is the electric field strength (in volts per centimeter) and t is the time required for the sample to migrate from the inlet to the detector (in seconds).

The observed mobility is the algebraic sum of the true mobility of the hairpin, μ, and the mobility caused by the electroosmotic flow (EOF) of the solvent, μ_{EOF}, as shown in eq 3:

$$\mu_{obs} = \mu + \mu_{EOF} \tag{3}$$

Because the residual EOF in coated capillaries is very small, corrections for μ_{EOF} are not needed for melting experiments. However, the residual EOF can vary slightly from one capillary to another. Therefore, to compare the mobilities measured in different capillaries, it is necessary to correct the observed mobilities for small differences in the residual μ_{EOF} of different capillaries. As described previously,[23] when the mobilities of a DNA hairpin and a marker (here T26) are measured in the same capillary at the same time, the difference in mobility between the two oligomers, $\Delta\mu$, is independent of μ_{EOF}. The mobility of each hairpin is then calculated from eq 4:

$$\mu = \langle\mu_{T26}\rangle + \Delta\mu \tag{4}$$

where $\langle\mu_{T26}\rangle$ is the average mobility of the marker under a given set of experimental conditions. Replicate experiments showed that the average standard deviation of the mobilities observed for the same sample on any given day varied by less than ±0.1%. The average day-to-day variation of the mobilities was less than ±0.3%. Such small variations in mobility are within the sizes of the symbols in the mobility plots illustrated below. For the sake of convenience, all mobilities are given in mobility units, m.u. (1 m.u. = 1×10^{-4} cm^2 V^{-1} s^{-1}).

Thermal Melting Studies. Thermal melting studies were conducted by measuring the mobilities of the target hairpin and T26 (co-injected into the capillary in the same solution) at temperatures ranging from 15 to 60 °C, the available range of the CE instrument. The capillary was allowed to equilibrate at each temperature for 3 min before the sample was injected; previous studies have shown that 3 min is adequate for temperature equilibration.[22,23] Mobility ratios were calculated by dividing the mobility of the hairpin by the mobility of T26 at each temperature, as described in more detail below. Plots of the mobility ratios as a function of temperature, called melting curves for the sake of brevity, were analyzed by global fits of the melting curves obtained at different Na^+ concentrations to a four-parameter Hill equation, using the algorithms given in SigmaPlot. The Hill equation is given in eq 5:

$$y = y_0 + \frac{ax^b}{c^b + x^b} \tag{5}$$

where y is the mobility ratio observed at temperature T, y_0 is the extrapolated mobility ratio at high temperatures, a is a constant that when added to y_0 is equal to the extrapolated mobility ratio at low temperatures, x is the temperature, c is the temperature at the midpoint of the transition, called the melting temperature, T_m, for the sake of brevity, and b describes the sigmoidal character of the transition. The melting curves of all hairpins were assumed to represent two-state conformational transitions that converged to a common limit, independent of Na^+ concentration, at high temperatures. To illustrate the precision of the analysis, the fitting parameters obtained from the global fits of the melting curves of the various hairpins in BGEs containing 225 mM Na^+ ions are given in Table S1 of the Supporting Information. The standard deviations of the melting temperatures are shown as error bars in the figures below when the uncertainties are larger than the sizes of the symbols.

RESULTS AND DISCUSSION

Measurement of Melting Curves. A typical electropherogram observed for a sample containing hp2 and T26, electrophoresed at 20 °C in a background electrolyte (BGE) containing 300 mM Na^+, is illustrated in Figure 1. The peaks are well-separated and approximately Gaussian in shape, with no significant molecular weight heterogeneity. The hairpins and T26 were added in different molar ratios so that the peaks could be identified by inspection. Similar electropherograms were observed for the other hairpins studied here (not shown).

No significant concentrations of homodimers were observed for any of the hairpins at any Na^+ concentration. Homodimer formation would be indicated by the presence of a second peak migrating faster than the hairpin peak, because duplex DNAs containing 26 bp have faster mobilities than hairpins or random

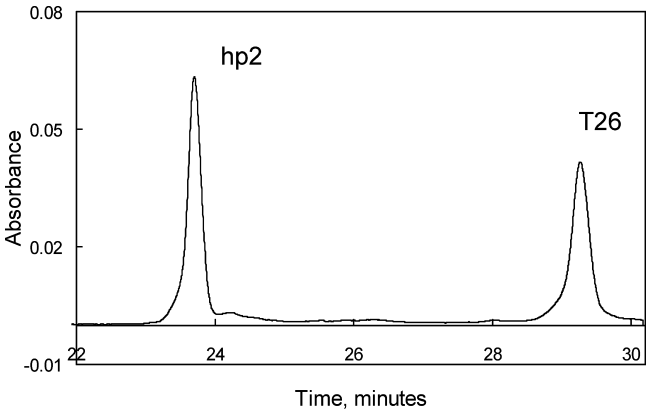

Figure 1. Typical electropherogram observed for hp2 and T26 at 20 °C in a BGE containing 300 mM Na^+. The absorbance, in arbitrary units, is plotted as a function of time after injection of the sample into the capillary. The electric field was 71 V/cm.

coils containing 26 nucleotides.[23] None of the electropherograms observed for hp1, hp2, or any of the sequence variants exhibited two peaks in addition to the marker peak. In addition, no significant variations in peak shape were observed when the hairpin concentration was varied by a factor of 2, again suggesting that significant concentrations of homodimers were not present in the solutions.

The mobilities observed for hp2 and T26 are plotted in Figure 2A as a function of temperature in a BGE containing 225 mM Na^+. The mobility of T26 (△) increases linearly with increasing temperature because of changes in the viscosity and dielectric constant of water with increasing temperature.[22,24,25,35] Because these values are known, the mobility of T26 at any temperature, T, can be predicted from the mobility measured at another temperature, e.g., 20 °C, using eq 6:

$$\mu_T = \mu_{20}\varepsilon_{rel}/\eta_{rel} \quad (6)$$

where μ_T is the mobility at temperature T, μ_{20} is the mobility observed at 20 °C, and ε_{rel} and η_{rel} are the ratios of the dielectric constant and the viscosity of water, respectively, at T and 20 °C. The temperature dependence of the mobility of T26 predicted by eq 3 is indicated by the solid line in Figure 2A. The good correspondence between the predicted and measured mobilities indicates that T26 does not undergo a conformational transition within the investigated temperature range. Hence, T26 is an unstructured random coil in solution, in agreement with other results in the literature.[24,36−39]

By contrast, the mobility of hp2 (● in Figure 2A) increases linearly with an increasing temperature only at temperatures between 15 and 30 °C. At higher temperatures, the mobility of hp2 gradually becomes lower than expected from the changes in the physical properties of water with increasing temperature, indicated by the dashed line. Hence, hp2 undergoes a conformational transition at high temperatures, most likely the denaturation of the hairpin to form a random coil.

To eliminate the effect of changes in the bulk properties of water on the observed mobilities and illustrate the melting transition more clearly, the ratio of the mobilities of hp2 and T26 can be plotted as a function of temperature, as shown in Figure 2B. The curved line corresponds to the fit of the mobility ratios to a four-parameter Hill equation. The midpoint of the transition, called the melting temperature, T_m, is 39.7 ± 0.3 °C. Similar results are obtained if the melting curves are plotted as the fractional hairpin concentration at each temperature,[40] using the solid and dashed lines in Figure 2A as the coil and hairpin baselines, respectively.[24] The resulting melting curve (not shown), analyzed with a four-parameter Hill equation, has a midpoint at 40.1 ± 0.5 °C, within experimental error of the value determined by the mobility ratio method. Hence, for the sake of simplicity, all thermal transitions were analyzed by the mobility ratio method.

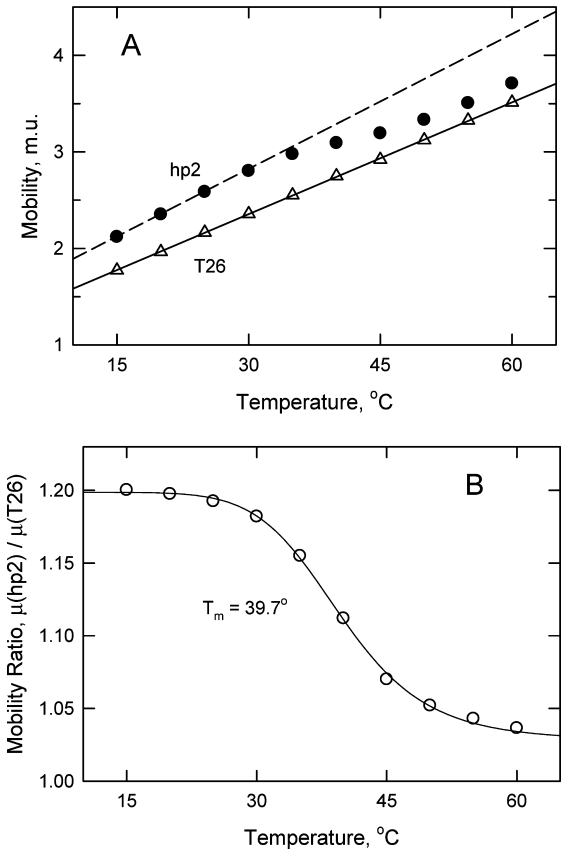

Figure 2. (A) Dependence of the mobility of hp2 (●) and T26 (△) on temperature in a BGE containing 225 mM Na^+. The solid and dashed lines indicate the expected increase in the mobility of each oligomer because of changes in the bulk properties of water with an increasing temperature. The mobilities are given in mobility units, m.u. (1 m.u. = 1×10^{-4} cm^2 V^{-1} s^{-1}). (B) Melting curve calculated for hp2 in the same BGE. The mobility ratio, μ(hp2)/μ(T26), is plotted as a function of temperature. The curved line corresponds to the fit obtained with a four-parameter Hill equation; the midpoint of the transition occurs at 39.7 ± 0.3 °C.

Melting Curves Observed for hp1 and hp2 at Different Na^+ Concentrations. Representative melting curves measured for hp2 as a function of temperature in BGEs containing 45−450 mM Na^+ are illustrated in Figure 3A. The melting curves are relatively sharp, with reasonably well-defined plateaus at both high and low temperatures. Differences in the low-temperature plateau values can be attributed to differences in the fractional hairpin population in the conformational ensemble at various salt concentrations. The melting curves appear to converge to the same limit at high temperatures, as expected if the random coil conformation is essentially independent of Na^+ concentration. The melting curves were therefore analyzed by a global fit of the data obtained at various Na^+ concentrations to a four-parameter Hill

dx.doi.org/10.1021/bi201263n | Biochemistry 2011, 50, 9148−9157

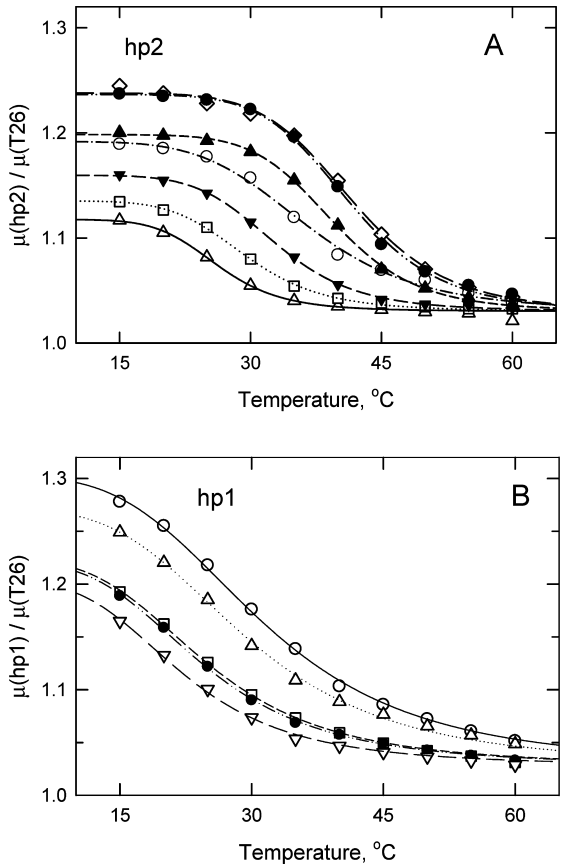

Figure 3. (A) Representative melting curves observed for hp2, where the mobility ratios, μ(hp2)/μ(T26), are plotted as a function of temperature for BGEs containing (◇) 450, (●) 300, (▲) 225, (○) 150, (▼) 112, (□) 75, and (△) 45 mM Na^+. (B) Representative melting curves observed for hp1 in BGEs containing (○) 600, (△) 450, (□) 375, (●) 300, and (▽) 225 mM Na^+. The curved lines in panels A and B were calculated from global fits of each set of melting curves to a four-parameter Hill equation, assuming that the mobility ratios extrapolate to a common value at high temperatures. The goodness of fit, r^2, is 0.998 for panel A and 0.997 for panel B.

equation, assuming that the limiting mobility ratio at high temperatures was independent of Na^+ concentration. The curved lines were calculated from the global fit.

Typical melting curves observed for hp1 in BGEs ranging from 225 to 600 mM Na^+ are illustrated in Figure 3B. The melting curves are broader than observed for hp2 and do not reach well-defined plateaus at low temperatures. The melting curves were analyzed by a global fit of the data to a four-parameter Hill equation, assuming that the mobility ratios reached a common limit at high temperatures. The curved lines were calculated from the global fit. To facilitate the comparison of the melting temperatures of hp1, hp2, and their sequence variants under a common set of conditions, the melting temperatures observed in BGEs containing 225 mM Na^+ are compiled in the third column of Table 1; the fitting parameters obtained at the same Na^+ concentration are given in Table S1 of the Supporting Information. The melting temperatures predicted by Mfold at the same Na^+ concentration are given in the fourth column of Table 1.

Attempts were made to measure melting curves for hp1 in BGEs containing <200 mM Na^+. However, the mobility ratios exhibited only a gradual decrease with an increasing temperature, instead of a sigmoidal transition. Similar gradual decreases in the mobility ratio were also observed for a sequence variant of hp1 in which the first two residues in the sequence were interchanged, preventing the formation of a stable 5 bp stem (hp1-no-beacon). The combined results indicate that hp1 does not form a stable hairpin in solutions containing less than ~200 mM Na^+.

The limiting mobility ratios observed for hp1 and hp2 at high temperatures were 1.028 and 1.030, respectively. The average mobility ratio observed at high temperatures for all sequence variants studied here was 1.028 ± 0.003. Because the limiting mobility ratios were greater than 1.00, the mobilities of the denatured hairpins at high temperatures were ~3% greater than the mobility of T26 at the same temperature. The results are consistent with previous studies indicating that small single-stranded thymine oligomers have somewhat lower electrophoretic mobilities than other single-stranded DNAs containing the same number of nucleotides.[41]

Dependence of the Melting Temperatures of hp1 and hp2 on Na^+ Concentration. The melting temperatures (T_m) observed for hp1 and hp2 increased approximately linearly with the logarithm of the Na^+ ion concentration, as shown in Figure 4A. Similar results have been observed for other DNA hairpins.[22,42−46] The melting temperatures observed for hp2 (△) are reasonably close to the values predicted by Mfold,[30,31] as shown by comparing the empty triangles with the dashed line. However, the melting temperatures observed for hp1 (○) are ~18 °C lower than those observed for hp2 at all Na^+ concentrations for which a stable hairpin is formed and ~20 °C lower than those predicted by Mfold (−·−). Hence, despite the similarity of the melting temperatures predicted by Mfold, hp1 is significantly less stable than hp2.

Increasing the GC Content of the hp1 Stem. To improve our understanding of the anomalously low melting temperature of hp1, the stability of the stem was increased by increasing the GC content, creating hp1-stable-stem (Table 1). Melting curves similar to those in Figure 3 were obtained for hp1-stable-stem (not shown); the dependence of the melting temperature on the logarithm of the Na^+ ion concentration is illustrated by the empty squares in Figure 4B. Not surprisingly, hp1-stable-stem forms a stable hairpin at Na^+ concentrations much lower than those observed for hp1. Although the melting temperatures of hp1-stable-stem (□) are ~20 °C higher than those observed for hp1 (○), they are ~10 °C lower than those predicted by Mfold, as shown by comparing the empty squares with the dashed line. Hence, the loop sequence of hp1 and/or the nucleotides in the stem−loop junction must be responsible for the anomalously low stability of hp1.

Variations in the Stem−Loop Junction. To test the importance of the nucleotides at the stem−loop junctions in hp1 and hp2, the two adenine residues located at the base of the hp1 loop were replaced with thymine residues (hp1-TT-loop-close), and the two thymine residues at the base of the hp2 loop were replaced with adenine residues (hp2-AA-loop-close). A third construct was also created in which the residues in the stem of hp1 were rearranged so that the closing base pair in the stem was GC instead of AT (hp1-GC-stem-close). Melting curves were measured for these constructs at various Na^+ concentrations; the melting temperatures increased linearly with log[Na^+] as observed for hp1 and hp2 (not shown). The melting temperature increased by ~10 °C when thymine residues replaced the adenine residues at the base of the hp1 loop or when the base pair at the top of the hp1 stem was changed from AT to GC, as shown in Table 1 for BGEs

dx.doi.org/10.1021/bi201263n | Biochemistry 2011, 50, 9148−9157

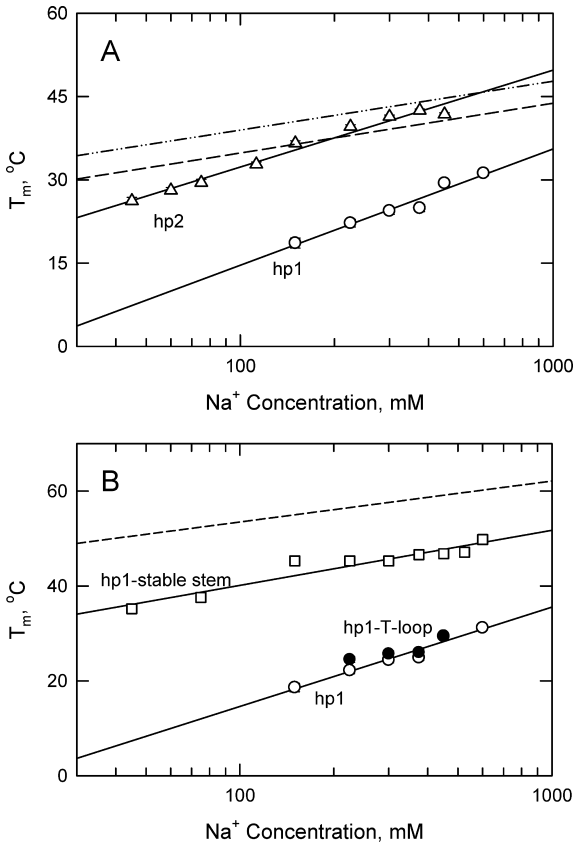

Figure 4. (A) Dependence of the melting temperatures observed for (○) hp1 and (△) hp2 on the logarithm of the Na^+ concentration. In this and subsequent figures, error bars are shown if they are larger than the sizes of the symbols. The solid lines were drawn by linear regression (r^2 = 0.958 and 0.976 for hp1 and hp2, respectively). The dotted–dashed and dashed lines correspond to the melting temperatures predicted for hp1 and hp2, respectively, by Mfold. (B) Comparison of the melting temperatures observed for (○) hp1, (□) hp1-stable-stem, and (●) T-loop hairpin at different Na^+ concentrations. The solid lines were drawn by linear regression (r^2 = 0.958 and 0.901 for hp1 and hp1-stable-stem, respectively). The dashed line corresponds to the melting temperatures predicted by Mfold for hp1-stable-stem.

containing 225 mM Na^+. The melting temperature of hp2 decreased by ~3 °C when the loop closing residues were changed from thymine to adenine, as also shown in Table 1. The results are consistent with other studies showing that hairpins with loops closed by thymine residues or with stems closed by GC base pairs are more stable than similar hairpins with loops closed by adenine residues or stems closed by AT base pairs.[19,20,47−55] However, the results also suggest that these variations in the stem–loop junction are too small to explain the large difference in stability between hp1 and hp2.

Replacing the Loops of hp1 and hp2 with an Equal Number of Thymine Residues. Melting curves were measured for an oligomer in which the loops of hp1 and hp2 were replaced with an equal number of thymine residues, keeping the stem residues constant (T-loop hairpin). Within experimental error, the melting temperatures of the T-loop hairpin were identical to those of hp1, as shown by comparing the empty and filled circles in Figure 4B. Because the thymine loops in molecular beacon-like hairpins are flexible coils,[56] the results suggest that the hp1 loop is unstructured, with relatively few base–base stacking interactions. By inference, the results also suggest that the hp2 loop must be highly structured, with significant base stacking and/or base pairing interactions.

Placing Tandem GA Residues in the Loop of hp1. One obvious difference between the loops of hp1 and hp2 is the presence of tandem GA residues on opposite sides of the hp2 loop, relatively close to the stem–loop junction. In principle, these residues could interact, possibly by forming non-Watson–Crick GA base pairs across the loop.[57−60] To test the importance of the tandem GA residues in the hp2 loop to hairpin stability, the corresponding TC residues in the hp1 loop were replaced with tandem GA residues, creating the sequence variant hp1-2GA. As shown in Figure 5, the melting

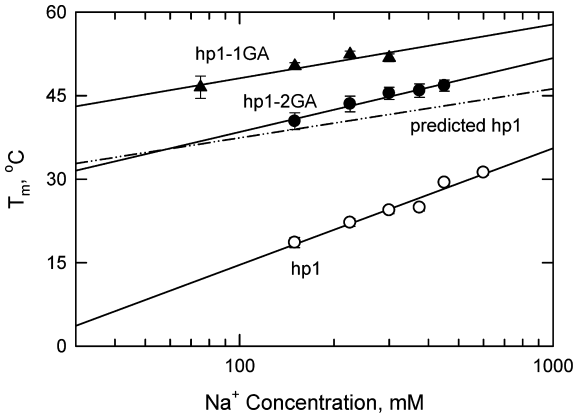

Figure 5. Melting temperatures observed for sequence variants of hp1 containing tandem GA residues in the loop: (●) hp1-2GA, (▲) hp1-1GA, and (○) hp1. The lines were drawn by linear regression (r^2 = 0.969, 0.904, and 0.958 for hp1-2GA, hp1-1GA, and hp1, respectively). For comparison, the melting temperatures predicted by Mfold for hp1 are indicated by the dashed–dotted line.

temperatures observed for hp1-2GA (●) were ~20 °C higher than those observed for hp1 (○) at all Na^+ concentrations and approximately equal to the melting temperatures predicted for hp1 by Mfold (dashed–dotted line).

If only one of the tandem TC residues in the hp1 loop was replaced by tandem GA residues, creating hp1-1GA, the stability of the hairpin was increased even more, as shown by the filled triangles in Figure 5. The melting temperatures of hp1-1GA are predicted well by Mfold, as shown in Table 1. The Mfold-predicted structure of hp1-1GA is that of a hairpin with 9 bp in the stem (plus one mismatch) and a loop containing six residues, as shown in Figure 6A (right-most structure). By contrast, the structures predicted by Mfold for hp1 and hp2 are hairpins with identical 5 bp stems and open loops containing 16 nucleotides, as shown in the left and middle structures in Figure 6A. The increased stability of hp1-1GA is thus due to the increased length of the stem because eight of the residues in the hp1 loop have formed stable Watson–Crick base pairs in hp1-1GA.

The marked increase in the stability of hp1 when two pairs of tandem GA residues are incorporated in the loop suggests that the tandem GA residues in the loops of hp1-2GA, hp2, and hp2-AA-stem-close interact with each other across the loop, effectively increasing the length of the stem, as suggested by the structures shown in Figure 6B. The results also suggest that loop compaction is implicit in the Mfold algorithm, because the melting temperatures of hp2, hp2-AA-loop-close, hp1-1GA, and hp1-2GA are reasonably well predicted by Mfold (Table 1),

dx.doi.org/10.1021/bi201263n | Biochemistry 2011, 50, 9148–9157

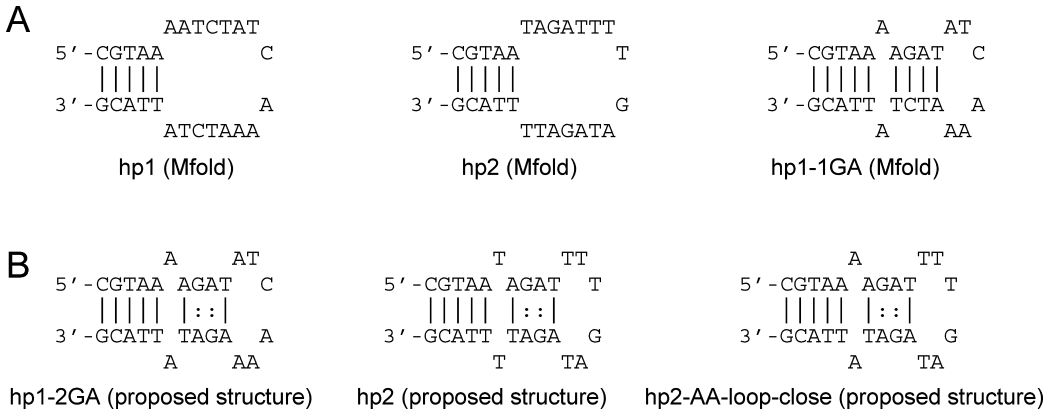

Figure 6. (A) Structures predicted by Mfold for hp1, hp2 and hp1-1GA (from left to right, respectively). The complete set of structures predicted by Mfold for the hp1 and hp2 sequence variants is given in Figure S1 of the Supporting Information. (B) Proposed interactions between tandem GA residues in the loops of hp1-2GA, hp2, and hp2-AA-loop-close (from left to right, respectively).

while the melting temperatures of hairpins with unstructured loops, such as hp1 and the T-loop hairpin, are poorly predicted by Mfold.

Eliminating the Tandem GA Residues in the hp2 Loop. If adding tandem GA residues to the hp1 loop increased hairpin stability, eliminating the tandem GA residues from the hp2 loop would be expected to decrease hairpin stability. The tandem GA residues in the hp2 loop were therefore replaced with tandem TC residues, creating the sequence variant hp2-2TC. Surprisingly, however, the melting temperatures of hp2-2TC were very close to those observed for hp2, as shown in Table 1. The conformation predicted for hp2-2TC by Mfold is that of a hairpin with four thymine residues in the loop and a stem containing 9 bp and a 4 nt bulge, as shown in Figure S1 of the Supporting Information. The melting temperatures observed for hp1-2TC agree with the values predicted by Mfold (Table 1).

A second sequence variant of hp2 was also created in which the adenine residues near the base of the loop were changed to guanines, eliminating any possible interactions between tandem GA residues on opposite sides of the loop. The melting temperatures of this construct, called hp2-3G, were equal to those of hp1-TT-loop-close, as shown in Table 1 for BGEs containing 225 mM Na^+. Hence, eliminating the tandem GA residues on opposite sides of the hp2 loop created a hairpin with an open loop structure, similar to that of hp1 and the T-loop hairpin. The combined results suggest that the thermal stability of molecular beacon-type hairpins is determined primarily by the compactness of the loop. Loop compactness can be enhanced by having thymine residues at the base of the loop instead of adenine residues or by interactions between tandem GA residues located on opposite sides of the loop.

Comparison of the Free Solution Mobility with Hairpin Stability. If the thermal stability of molecular beacon-type hairpins is determined by loop compactness, there should be a correlation between the free solution mobility observed at 20 °C and the melting temperatures observed under a given set of experimental conditions. Such a correlation is shown in Figure 7 for hp1, hp2, and their sequence variants in BGEs containing 225 mM Na^+; the mobilities observed at 20 °C are given in the last column of Table 1. Similar results are observed at other Na^+ concentrations (not shown).

The free solution mobilities observed at 20 °C are determined by three factors: the effective charge of the oligomer, its frictional coefficient, and the relative proportion of hairpins in the conformational ensemble at that temperature.[23,24] Because all three factors affect the observed mobility, the free solution mobility at 20 °C is a good predictor of hairpin formation.

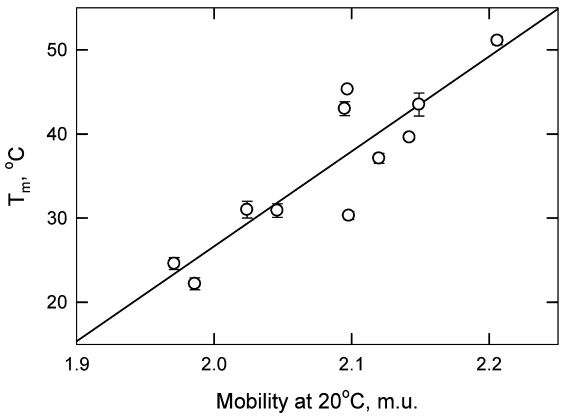

Figure 7. Correlation between the melting temperatures observed for hp1, hp2, and their sequence variants and the free solution mobilities observed at 20 °C in BGEs containing 225 mM Na^+. The line was drawn by linear regression (r^2 = 0.787).

Stabilization of Molecular Beacon-like Hairpins by Na^+. At a constant temperature, the mobility of DNA decreases approximately linearly with the logarithm of cation concentration, as shown in Figure 8A for T26. Similar results have been observed for other DNA oligomers[23,24,35,42,43,61−63] and are expected theoretically.[35,45] However, the melting curves in Figure 3 suggest that the conformational ensembles present at low temperatures contain different populations of hairpins in BGEs containing low concentrations of Na^+. To analyze the effect of Na^+ concentration on hairpin stability, the mobility of T26 was subtracted from the mobilities of the hairpins to eliminate the dependence of hairpin mobility on Na^+ concentration. The mobility differences observed for hp1, hp2, hp1-2GA, and hp1-no-beacon are illustrated in Figure 8B. The mobility differences observed for hp1-no-beacon were essentially independent of Na^+ concentration and reflect differences in the intrinsic mobilities of thymine oligomers and other DNAs containing the same number of nucleotides.[41]

However, different results were observed for hp1, hp2, and hp1-2GA, as also shown in Figure 8B. The mobility differences

dx.doi.org/10.1021/bi201263n | Biochemistry 2011, 50, 9148−9157

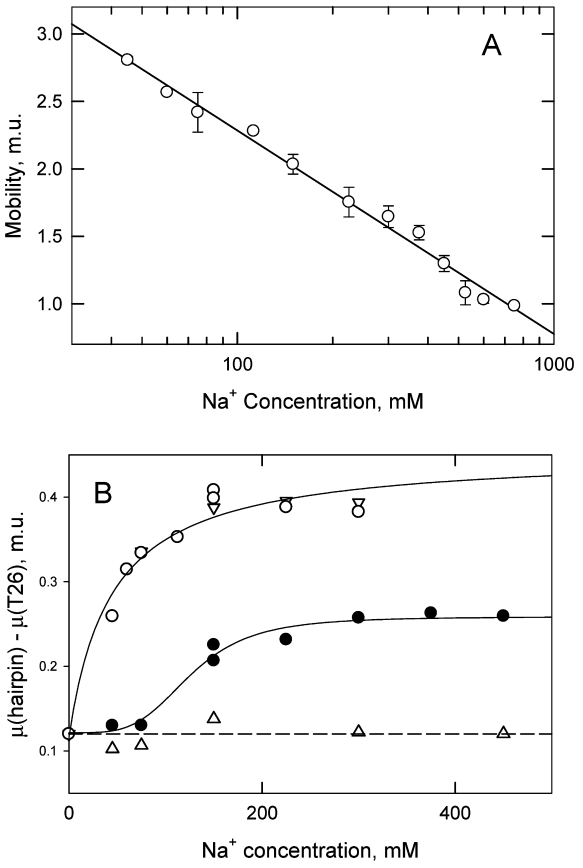

Figure 8. (A) Dependence of the mobility of T26 (○) on the logarithm of the Na^+ concentration at 20 °C. The error bars correspond to the standard deviation of multiple measurements taken at each Na^+ concentration. The line was drawn by linear regression (r^2 = 0.989). (B) Dependence of the difference in mobility between representative hairpins and T26, measured at 20 °C in BGEs containing various Na^+ concentrations: (●) hp1, (○) hp2, (▽) hp1-2GA, and (△) hp1-no-beacon. The horizontal dashed line corresponds to the average mobility difference between T26 and hp1-no-beacon (0.120 ± 0.013 m.u.) and represents the intrinsic mobility difference between T26 and the unstructured hairpins at 20 °C. The bottom curved line corresponds to a four-parameter sigmoidal fit of the hp1 data, with a midpoint at 126 ± 9 mM Na^+ (r^2 = 0.983). The top curved line corresponds to a three-parameter hyperbolic fit of the data obtained for hp2 and hp1-2GA, with a midpoint at 44 ± 15 mM Na^+ (r^2 = 0.953).

observed for hp1 increased sigmoidally with an increasing Na^+ concentration, with a transition midpoint at 126 ± 9 mM Na^+. The mobility differences observed for hp2 and hp1-2GA can be fitted with a hyperbolic binding curve with a midpoint at 44 ± 15 mM. The combined results suggest that the conformations of molecular beacon-like hairpins are stabilized by binding Na^+ ions. The more stable hairpins have a stronger affinity for Na^+ ions and reach saturation binding levels at lower Na^+ concentrations.

CONCLUDING REMARKS

These studies have shown that two complementary 16-nucleotide oligomers, called hp1 and hp2, exhibit different free solution electrophoretic mobilities at 20 °C and very different thermal stabilities, suggesting that they have different conformations in solution. The less stable hairpin, hp1, appears to contain a relatively unstructured loop with very few base–base stacking interactions. By contrast, the loop of the more stable hairpin, hp2, appears to be compacted by interactions between tandem GA residues on opposite sides of the loop that increase the mobility of this hairpin and increase its stability. Placing tandem GA residues on opposite sides of the hp1 loop makes the modified hairpin (hp1-2GA) as stable as hp2; eliminating the tandem GA residues in the hp2 loop decreases the stability of the modified hairpin (hp2-3G), making it equal to that of the hp1 sequence variant with thymine loop-closing residues (hp1-TT-loop-close).

Tandem GA base pairs are known to stabilize duplex DNAs by forming sheared base pairs with extensive cross-strand base stacking interactions.[57−60,64−69] However, it seems unlikely that the tandem GA base pairs in the loops of hp1-2GA, hp2, and hp2-AA-loop-close have the sheared conformation, because the tandem GA residues in the loops are preceded by adenine and followed by thymine residues. The sheared GA base pairs previously observed in duplex DNAs have been found only in the pyrimidine-GA-purine sequence context.[60,65,67,69,70] Further studies will be needed to determine the precise nature of the interactions between the tandem GA residues on opposite sides of the loops in hp1-2GA, hp2, and hp2-AA-loop-close.

The stability of hp2 is reasonably well predicted by the popular structure-prediction program Mfold.[30,31] However, the Mfold-predicted melting temperatures for hp1 are ∼20 °C higher than the observed melting temperatures at all Na^+ concentrations for which hp1 forms a stable hairpin. The discrepancy appears to be due to the fact that the hp1 loop is relatively unstructured, with few base–base stacking interactions; base stacking in hairpin loops therefore appears to be an implicit assumption in the Mfold algorithm. Base pairing interactions between pairs of nucleotides on opposite sides of large hairpin loops appear to contribute importantly to loop compaction and the stability of molecular beacon-like hairpins.

ASSOCIATED CONTENT

Supporting Information

Structures predicted by Mfold for hp1, hp2, and their sequence variants and proposed interactions between the tandem GA residues on opposite sides of the loops in hp2, hp1-2GA, and hp2-AA-stem-close (Figure S1) and fitting parameters obtained from global fits of the melting curves of the various hairpins to a four-parameter Hill equation in BGEs containing 225 mM Na^+ ions (Table S1). This material is available free of charge via the Internet at http://pubs.acs.org.

AUTHOR INFORMATION

Corresponding Author

*Telephone: (319) 335-7896. Fax: (319) 335-9570. E-mail: nancy-stellwagen@uiowa.edu.

Present Address

†G382 Toad Hall, Building 30, Kingsley Street, Acton, ACT, 2601, Australia.

Funding

This work was supported in part by Grant CHE0748271 from the Analytical and Surface Chemistry Program of the National Science Foundation (to N.C.S.).

ACKNOWLEDGMENTS

Helpful discussions with Earle Stellwagen and Paul Barnard are gratefully acknowledged.

■ ABBREVIATIONS

BGE, background electrolyte; CE, capillary electrophoresis; EOF, electroosmotic flow; m.u., mobility unit (1 m.u. = 1 × 10^{-4} cm^2 V^{-1} s^{-1}).

■ REFERENCES

(1) Ricelli, P. V., Merante, F., Leung, K. T., Bortolin, S., Zastawny, R. L., Janeczko, R., and Benight, A. S. (2001) Hybridization of single-stranded DNA targets to immobilized complementary DNA probes: Comparison of hairpin versus linear capture probes. *Nucleic Acids Res. 29*, 996−1004.

(2) Seeman, N. C. (2005) From genes to machines: DNA nanomechanical devices. *Trends Biochem. Sci. 30*, 119−125.

(3) Zhang, C., Su, M., He, Y., Zhao, X., Fang, P.-a., Ribbe, A. E., Jiang, W., and Mao, C. (2008) Conformational flexibility facilitates self-assembly of complex DNA nanostructures. *Proc. Natl. Acad. Sci. U.S.A. 105*, 10665−10669.

(4) Service, R. F. (2011) DNA nanotechnology grows up. *Science 332*, 1140−1143.

(5) Tsourkas, A., Behlke, M. A., Rose, S. D., and Bao, G. (2003) Hybridization kinetics and thermodynamics of molecular beacons. *Nucleic Acids Res. 31*, 1319−1330.

(6) Bonnet, G., Krichevsky, O., and Libchaber, A. (1998) Kinetics of conformational fluctuations in DNA hairpin-loops. *Proc. Natl. Acad. Sci. U.S.A. 95*, 8602−8606.

(7) Tan, W., Wang, K., and Drake, T. J. (2004) Molecular beacons. *Curr. Opin. Chem. Biol. 8*, 547−553.

(8) Tyagi, S., and Kramer, F. R. (1996) Molecular beacons: Probes that fluoresce upon hybridization. *Nat. Biotechnol. 14*, 303−308.

(9) Antao, V. P., and Tinoco, I. Jr. (1992) Thermodynamic parameters for loop formation in RNA and DNA hairpin tetraloops. *Nucleic Acids Res. 20*, 819−824.

(10) SantaLucia, J. Jr. (1998) A unified view of polymer, dumbbell, and oligonucleotide DNA nearest-neighbor thermodynamics. *Proc. Natl. Acad. Sci. U.S.A. 95*, 1460−1465.

(11) Owczarzy, R., Vallone, P. M., Gallo, F. J., Paner, T. M., Lane, M. J., and Benight, A. S. (1997) Predicting sequence-dependent melting stability of short duplex DNA oligomers. *Biopolymers 44*, 217−239.

(12) SantaLucia, J. Jr., and Hicks, D. (2004) The thermodynamics of DNA structural motifs. *Annu. Rev. Biophys. Biomol. Struct. 33*, 415−440.

(13) Owczarzy, R., You, Y., Moreira, B. G., Manthey, J. A., Huang, L., Behlke, M. A., and Walder, J. A. (2004) Effects of sodium ions on DNA duplex oligomers: Improved predictions of melting temperatures. *Biochemistry 43*, 3537−3554.

(14) Peyret, N. (2000) Prediction of nucleic acid hybridization: Parameters and algorithms. Ph.D. Dissertation, Wayne State University, Detroit.

(15) Allawi, H. T., and SantaLucia, J. Jr. (1997) Thermodynamics and NMR of internal G·T mismatches in DNA. *Biochemistry 36*, 10581−10594.

(16) Allawi, H. T., and SantaLucia, J. Jr. (1998) Nearest neighbor thermodynamic parameters for internal G·A mismatches in DNA. *Biochemistry 37*, 2170−2179.

(17) Allawi, H. T., and SantaLucia, J. Jr. (1998) Thermodynamics of internal C·T mismatches in DNA. *Nucleic Acids Res. 26*, 2694−2710.

(18) Peyret, N., Seneviratne, P. A., Allawi, H. T., and SantaLucia, J. Jr. (1999) Nearest-neighbor thermodynamics and NMR of DNA sequences with internal A·A, C·C, G·G, and T·T mismatches. *Biochemistry 38*, 3468−3477.

(19) Senior, M. M., Jones, R. A., and Breslauer, K. J. (1988) Influence of loop residues on the relative stabilities of DNA hairpin structures. *Proc. Natl. Acad. Sci. U.S.A. 85*, 6242−6246.

(20) Vallone, P. M., Paner, T. M., Hilario, J., Lane, M. J., Faldasz, B. D., and Benight, A. S. (1999) Melting studies of short DNA hairpins: Influence of loop sequence and adjoining base pair identity on hairpin thermodynamic stability. *Biopolymers 50*, 425−442.

(21) You, Y., Tataurov, A. V., and Owczarzy, R. (2011) Measuring thermodynamic details of DNA hybridization using fluorescence. *Biopolymers 95*, 472−486.

(22) Stellwagen, E., Renze, A., and Stellwagen, N. C. (2007) Capillary electrophoresis is a sensitive monitor of the hairpin-random coil transition in DNA oligomers. *Anal. Biochem. 365*, 103−110.

(23) Stellwagen, E., Abdulla, A., Dong, Q., and Stellwagen, N. C. (2007) Electrophoretic mobility is a reporter of hairpin structure in single-stranded DNA oligomers. *Biochemistry 46*, 10931−10941.

(24) Stellwagen, E., Muse, J. M., and Stellwagen, N. C. (2011) Monovalent cation size and DNA conformational stability. *Biochemistry 50*, 3084−3094.

(25) Viovy, J.-L. (2000) Electrophoresis of DNA and other polyelectrolytes: Physical mechanisms. *Rev. Mod. Phys. 72*, 813−872.

(26) Zeng, Y., Montrichok, A., and Zocchi, G. (2004) Bubble nucleation and cooperativity in DNA melting. *J. Mol. Biol. 339*, 67−75.

(27) Zeng, Y., and Zocchi, G. (2006) Mismatches and bubbles in DNA. *Biophys. J. 90*, 4522−4529.

(28) Stellwagen, N. C. (1997) DNA mobility anomalies are determined primarily by polyacrylamide gel concentration, not gel pore size. *Electrophoresis 18*, 34−44.

(29) Stellwagen, N. C. (2009) Effect of the matrix on DNA electrophoretic mobility. *J. Chromatogr., A 1216*, 1917−1929.

(30) Zuker, M. (2003) Mfold web server for nucleic acid folding and hybridization prediction. *Nucleic Acids Res. 31*, 3406−3415.

(31) Markham, N. R., and Zuker, M. (2005) DINAMelt web server for nucleic acid melting prediction. *Nucleic Acids Res. 33*, W577−W581.

(32) Stellwagen, E., Dong, Q., and Stellwagen, N. C. (2007) Quantitative analysis of monovalent counterion binding to random-sequence, double-stranded DNA using the replacement ion method. *Biochemistry 46*, 2050−2058.

(33) Stellwagen, E., Lu, Y. J., and Stellwagen, N. C. (2005) Curved DNA molecules migrate anomalously slowly in free solution. *Nucleic Acids Res. 33*, 4425−4432.

(34) Stellwagen, N. C., Gelfi, C., and Righetti, P. G. (1997) The free solution mobility of DNA. *Biopolymers 42*, 687−703.

(35) Manning, G. S. (1981) Limiting laws and counterion condensation in polyelectrolyte solutions. 7. Electrophoretic mobility and conductance. *J. Phys. Chem. 85*, 1506−1515.

(36) Camerman, N., Fawcett, J. K., and Camerman, A. (1976) Molecular structure of a deoxyribose-dinucleotide, sodium thymidylyl-(5′-3′)-thymidylate-(5′) hydrate (pTpT), and a possible structural model for polythymidylate. *J. Mol. Biol. 107*, 601−621.

(37) Murphy, M. C., Rasmik, I., Cheng, W., Lohman, T. M., and Ha, T. (2004) Probing single-stranded DNA conformational flexibility using fluorescence spectroscopy. *Biophys. J. 86*, 2530−2537.

(38) Saenger, W. (1983) *Principles of Nucleic Acid Structure*, Springer-Verlag, New York.

(39) Doose, S., Barsch, H., and Sauer, M. (2007) Polymer properties of polythymine as revealed by translational diffusion. *Biophys. J. 93*, 1224−1234.

(40) Marky, L. A., and Breslauer, K. J. (1987) Calculating thermodynamic data for transitions of any molecularity from equilibrium melting curves. *Biopolymers 26*, 1601−1620.

(41) Biyani, M., and Nishigaki, K. (2003) Sequence-specific and nonspecific mobilities of single-stranded oligonucleotides observed by changing the borate buffer concentration. *Electrophoresis 24*, 628−633.

(42) Rentzeperis, D., Kharakoz, D. P., and Marky, L. A. (1991) Coupling of sequential transitions in a DNA double hairpin: Energetics, ion binding, and hydration. *Biochemistry 30*, 6276−6283.

(43) Rentzeperis, D., Ho, J., and Marky, L. A. (1993) Contribution of loops and nicks to the formation of DNA dumbbells: Melting behavior and ligand binding. *Biochemistry 32*, 2564−2572.

(44) Rentzeperis, D., Alessi, K., and Marky, L. A. (1993) Thermodynamics of DNA hairpins: Contribution of loop size to hairpin stability and ethidium binding. *Nucleic Acids Res. 21*, 2683−2689.

(45) Shkel, I. A., and Record, M. T. Jr. (2004) Effect of the number of nucleic acid oligomer charges on the salt dependence of stability (ΔG°_{37}) and melting temperature (T_m): NLPB analysis of experimental data. *Biochemistry 43*, 7090−7101.
(46) Mandell, K. E., Vallone, P. M., Owczarzy, R., Riccelli, P. V., and Benight, A. S. (2006) Studies of DNA dumbbells. VIII. Melting analysis of DNA dumbbells with dinucleotide repeat stem sequences. *Biopolymers 82*, 199−221.
(47) Hilbers, C. W., Haasnoot, C. A. G., de Bruin, S. H., Joordens, J. J. M., van der Marel, G. A., and van Boom, J. H. (1985) Hairpin formation in synthetic oligonucleotides. *Biochimie 67*, 685−695.
(48) Haasnoot, C. A. G., Hilbers, C. W., van der Marel, G. A., van Boom, J. H., Singh, U. C., Pattabiraman, N., and Kollman, P. A. (1986) On loop folding in nucleic acid hairpin-type structures. *J. Biomol. Struct. Dyn. 3*, 843−857.
(49) Kuznetsov, S. V., Shen, Y., Benight, A. S., and Ansari, A. (2001) A semiflexible polymer model applied to loop formation in DNA hairpins. *Biophys. J. 81*, 2864−2875.
(50) Paner, T. M., Riccelli, P. V., Owczarzy, R., and Benight, A. S. (1996) Studies of DNA dumbbells. VI. Analysis of optical melting curves of dumbbells with a sixteen-base pair duplex stem and end-loops of variable size and sequence. *Biopolymers 39*, 779−793.
(51) Moody, E. M., and Bevilacqua, P. C. (2003) Thermodynamic coupling of the loop and stem in unusually stable DNA hairpins closed by CG base pairs. *J. Am. Chem. Soc. 125*, 2032−2033.
(52) Moody, E. M., and Bevilacqua, P. C. (2004) Structural and energetic consequences of expanding a highly cooperative stable DNA hairpin loop. *J. Am. Chem. Soc. 126*, 9570−9577.
(53) Williamson, J. R., and Boxer, S. G. (1989) Multinuclear NMR studies of DNA hairpins. 2. Sequence-dependent structural variations. *Biochemistry 28*, 2831−2836.
(54) Nakano, M., Moody, E. M., Liang, J., and Bevilacqua, P. C. (2002) Selection for thermodynamically stable DNA tetraloops using temperature gradient gel electrophoresis reveals four motifs: d(cGCCAg), d(cGNABg), d(cCNNGg), and d(gCNNGc). *Biochemistry 41*, 14281−14292.
(55) Hirao, I., Nishimura, Y., Tagawa, Y.-i., Watanabe, K., and Miura, K.-i. (1992) Extraordinarily stable mini-hairpins: Electrophoretical and thermal properties of the various sequence variants of d(GCGAAAGC) and their effect on DNA sequencing. *Nucleic Acids Res. 20*, 3891−3896.
(56) Goddard, N. L., Bonnet, F., Krichevsky, O., and Libchaber, A. (2000) Sequence dependent rigidity of single stranded DNA. *Phys. Rev. Lett. 85*, 2400−2403.
(57) Li, Y., Zon, G., and Wilson, W. D. (1991) NMR and molecular modeling evidence for a G·A mismatch base pair in a purine-rich DNA duplex. *Proc. Natl. Acad. Sci. U.S.A. 88*, 26−30.
(58) Chou, S.-H., Cheng, J.-W., and Reid, B. R. (1992) Solution structure of $[d(ATGAGCGAATA)]_2$. Adjacent G·A mismatches stabilized by cross-strand base-stacking and B_{II} phosphate groups. *J. Mol. Biol. 228*, 138−155.
(59) Lane, A., Martin, S. R., Ebel, S., and Brown, T. (1992) Solution conformation of a deoxynucleotide containing tandem G·A mismatched base pairs and 3′-overhanging ends in $d(GTGAACTT)_2$. *Biochemistry 31*, 12087−12095.
(60) Katahira, M., Sato, H., Mishima, K., Uesugi, S., and Fujii, S. (1993) NMR studies of G:A mismatches in oligodeoxyribonucleotide duplexes modelled after ribozymes. *Nucleic Acids Res. 21*, 5418−5424.
(61) Williams, A. P., Longfellow, C. E., Freier, S. M., Kierzek, R., and Turner, D. H. (1989) Laser temperature-jump, spectroscopic, and thermodynamic study of salt effects on duplex formation by dGCATGC. *Biochemistry 28*, 4283−4291.
(62) Nakano, S.-i., Fujimoto, M., Hara, H., and Sugimoto, N. (1999) Nucleic acid duplex stability: Influence of base composition on cation effects. *Nucleic Acids Res. 27*, 2957−2965.
(63) Stellwagen, E., and Stellwagen, N. C. (2003) Probing the electrostatic shielding of DNA with capillary electrophoresis. *Biophys. J. 84*, 1855−1866.
(64) Chou, S.-H., Zhu, L., and Reid, B. R. (1997) Sheared purine·purine pairing in biology. *J. Mol. Biol. 267*, 1055−1067.
(65) Ebel, S., Lane, A. N., and Brown, T. (1992) Very stable mismatch duplexes: Structural and thermodynamic studies on tandem G·A mismatches in DNA. *Biochemistry 31*, 12083−12086.
(66) Lane, A., Ebel, S., and Brown, T. (1994) Properties of multiple G·A mismatches in stable oligonucleotide duplexes. *Eur. J. Biochem. 220*, 717−727.
(67) Greene, K. L., Jones, R. L., Li, Y., Robinson, H., Wang, A. H.-J., Zon, G., and Wilson, S. D. (1994) Solution structure of a GA mismatch DNA sequence, $d(CCATGAATGG)_2$, determined by 2D NMR and structural refinement methods. *Biochemistry 33*, 1053−1062.
(68) Katahira, M., Kanagawa, M., and Uesugi, S. (1994) Drastic difference in G:A base pairing between two consecutive G:A mismatches and a single G:A mismatch in DNA. *Nucleosides Nucleotides 13*, 1507−1515.
(69) Cheng, J.-W., Chou, S.-H., and Reid, B. R. (1992) Base pairing geometry in GA mismatches depends entirely on the neighboring sequence. *J. Mol. Biol. 228*, 1037−1041.
(70) Gao, Y.-G., Robinson, H., Sanishvili, R., Joachimiak, A., and Wang, A. H.-J. (1999) Structure and recognition of sheared tandem G·A base pairs associated with human centromere DNA sequence at atomic resolution. *Biochemistry 38*, 16452−16460.